

Damian Brewczyński  orcid.org/0000-0003-4763-138X
damian.brewczynski@mech.pk.edu.pl

Grzegorz Tora  orcid.org/0000-0002-2306-319X
tora@mech.pk.edu.pl

Laboratory of Techno-Climatic Research and Heavy Duty Machines, Faculty
of Mechanical Engineering, Cracow University of Technology

THE DESIGN AND ANALYSIS OF A MONOLITHIC GRIPPER MECHANISM FOR MICROSCOPIC TESTS

PROJEKT I ANALIZA MONOLITYCZNEGO MECHANIZMU CHWYTAKA DO BADAŃ MIKROSKOPOWYCH

Abstract

This paper presents the design and results of mechanism research. A lever mechanism for a gripper was made using monolith technology with constrictions in which the deformations correspond to limited rotation of the links. Unidirectional movement of the drive link is reduced and simultaneously converted into movement of the jaw clamp. Temporary centres of rotation were used to obtain the symmetrical and perpendicular movement of the two ends of the clamp in relation to its axis of symmetry. Computer simulations and tests were performed on a prototype of the gripper mechanism, confirming the adopted predictions of the device's operation.

Keywords: microgripper, kinematic analysis, prototype testing

Streszczenie

W pracy przedstawiono projekt i wyniki badań mechanizmu chwytaka. Mechanizm dźwigniowy robota wykonano w technologii monolitu z przewężeniami, w których odkształcenia odpowiadają ograniczonym obrotom ogniw. Jednokierunkowy ruch ogniw napędowego zostaje zredukowany, a następnie zamieniony na ruch zacisku szczęk. Wykorzystano chwilowe środki obrotu w celu uzyskania symetrycznego i prostopadłego ruchu dwóch końców zacisku względem jego osi symetrii. Wykonano symulacje komputerowe i badania na prototypie robota, potwierdzające przyjęte założenia pracy urządzenia.

Słowa kluczowe: mikrochwytak, analiza kinematyczna, badania prototypu

1. Introduction

Microgrippers, devices that perform clamp movement on a selected object, are used in microscopic work in micromechanics [1] and microbiology [2].

The dimensions of prokaryotic cells (1–10 μm) and eukaryotic cells (10–100 μm) show that the accuracy of microgripper movement should be of the order of at least 1 μm . Such a level of accuracy can be obtained using microgrippers with dimensions of several dozen microns. Another possibility of achieving this accuracy is the construction of a mechanism fitted in the microscope table which reduces the movement of the drive or hand to the movement of the jaw clamp with the expected accuracy and range.

The clamping motion of the jaws should be perpendicular and symmetrical to the axis of symmetry of the held part and should linearly depend on the motion of the drive [3]. It is also desirable to have a short delay time for the reaction of the jaws in relation to the operator's starting response. A common solution in this type of device is to make a mechanical part of the microgripper in the form of a monolith in which intentionally designed constrictions deform to a greater extent than the remaining part [4]. In a monolithic construction, the movement is performed due to material deformations. If you treat constrictions as kinematic rotary pairs and other elements as links, you can determine the mobility of the system, which has a significant impact on the precision and range of motion. It is desirable to have system in which for one drive has one degree of freedom. There is then an unequivocal, sufficiently precise movement of the links which is easy to determine based on the kinematic analysis. In the case of degree of mobility less than 1, a slight movement of the mechanism in the constrictions occurs with significant buckling of the links. For degree of mobility greater than one, link motions are obtained primarily by deformations in the constrictions; they depend on the balance of drive loads and deformation resistance. In this case, the monolith manufacturing inaccuracies strongly affect the accuracy of the movement.

A small range of motion, a resistance to deformation and low durability of neckings of the monolithic mechanism are the prices that are paid to eliminate slack and to implement smooth motion at the microscale.

Piezoelectric [5], electrostatic [2] or bimetallic [6] drives that require the use of an appropriate electronic control system are used to drive the microgrippers. A desirable feature of the microgripper is the use of force feedback [7], in which the resistance of the micro-object to the jaws, after being multiplied, is perceivable on the operator's joystick. Classic kinematic analysis of the monolithic mechanism should be supported by a MES analysis of monolith deformation [8]. However, obtaining accurate material data needed for such an analysis is very difficult with the use of PLA with partial filling in 3D printing technology. The use of this easy-to-use technology is designed to test whether it is suitable for the implementation of monolithic mechanisms that require micrometric accuracy of motion.

The aim of the publication is the experimental verification of the theoretical gear ratio and symmetry of movement of the jaws in the developed monolithic gripper construction with a drive performing micro-movements.

2. Gripper mechanism construction

The gripper mechanism structure was designed and made in the form of a monolith as shown in Fig. 1. The mechanism consists of a jaw clamping system (links 1–4) and a system that reduces the displacement of a link moved by the operator's hand. There are two reduction stages based on the one-sided lever principle. The first stage consists of links 4 and 5 and the second stage consists of links 6 and 7. The drive (not shown in the picture) moves point J on lever 7. The dimensions of the mechanism are 300 x 220 mm and the displacement of the J point on the millimetre scale results in the displacement of the extreme points of the jaws Q_1 and Q_2 on the micrometre scale.

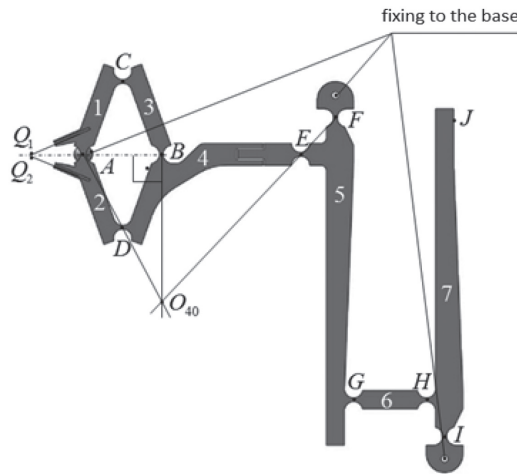


Fig. 1. Monolithic microgripper mechanism

Points Q_1 and Q_2 (Fig. 1) should move smoothly and symmetrically in the direction perpendicular to the axis of symmetry. Jaws 1 and 2 were connected to the base at joint A. Jaw 1, through joint C, is moved by double joint link 3. Jaw 2, through joint D, is moved by the triple joint link 4. The drive link is lever 7, the microgripper mechanism has one degree of freedom. The location of the double joint A on the axis of symmetry of the jaws causes the points of the ends of the jaws Q_1 and Q_2 , for the planned range of motion, to move on curves of a shape similar to the straight perpendicular axis of jaw symmetry. Providing a symmetrical movement of the jaws is possible when the centre of the pivot B moves along the axis of symmetry of the jaws. Then a straight line perpendicular to the axis of symmetry of the jaws passing through point B and the straight passing through the centres of joints A and D will intersect at point O_{40} (the momentary centre of rotation of the link 4 relative to the base 0). A construction requirement is that the points E and F of the link 5 are on one straight with O_{40} .

Due to the limitation of the print surface, the reduction and clamping parts were made separately and glued between levers 4 and 5.

3. Kinematic analysis of microgripper mechanism

In the kinematic analysis of the mechanism, the same calculation schemes are used several times. The first scheme applies to the rotation of the \hat{i} unit vector by the given angle κ to the position \hat{i}^* around the unit vector \hat{z} :

$$\hat{i}^* = \hat{i} \cos \kappa + (\hat{z} \times \hat{i}) \sin \kappa \quad (1)$$

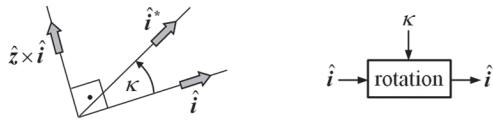


Fig. 2. Rotation of the unit vector by κ angle, symbolic rotation scheme

The second scheme applies to the designation of two unit vectors (\hat{i}_1, \hat{i}_2) included in the equation of the quadrilateral [9]:

$$l_1 \hat{i}_1 + l_2 \hat{i}_2 = l_3 \hat{i}_3 + l_4 \hat{i}_4 \quad (2)$$

There are two pairs of solutions distinguished by the parameter $k = -1, 1$:

$$\left. \begin{aligned} {}^k \hat{i}_1 &= A_1 \hat{s}_{34} + k \sqrt{1 - A_1^2} (\hat{z} \times \hat{s}_{34}) \\ {}^k \hat{i}_2 &= A_2 \hat{s}_{34} - k \sqrt{1 - A_2^2} (\hat{z} \times \hat{s}_{34}) \end{aligned} \right\} \quad (3)$$

where:

\hat{z} – a unit vector perpendicular to the plane of the quadrilateral,

$$s_{34} = |l_3 \hat{i}_3 + l_4 \hat{i}_4|, \hat{s}_{34} = \frac{l_3 \hat{i}_3 + l_4 \hat{i}_4}{s_{34}}, A_1 = \frac{l_1^2 + s_{34}^2 - l_2^2}{2l_1 s_{34}}, A_2 = \frac{l_2^2 + s_{34}^2 - l_1^2}{2l_2 s_{34}}.$$

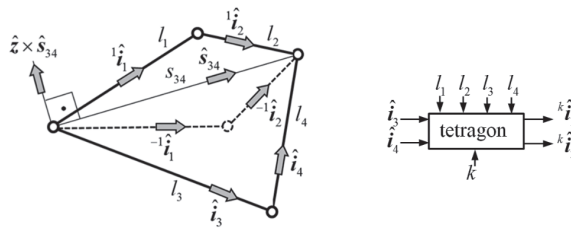


Fig. 3. Quadrilateral unit vectors, symbolic calculation scheme

3.1. Link orientations

Orientations of the links of the mechanism are represented by the unit vectors and depend upon the angular position of the drive link. The operator performs an angular movement of link 7, which is reduced by a group of two single-sided levers connected in series to form two

articulated quadrilaterals as shown in Fig. 4. An algorithm for determining the orientation of gripper mechanism links, shown in Fig. 5. developed on the basis of Fig. 4. and equations of three quadrangles was created:

$$FIHG \rightarrow l_{FG}\hat{i}_5^* + l_{GH}\hat{i}_6^* = l_{FI}\hat{i}_0^* + l_{IH}\hat{i}_7^* \quad (4)$$

$$ADEF \rightarrow l_{AD}\hat{i}_2^* + l_{DE}\hat{i}_4^* = l_{AF}\hat{i}_0^* + l_{FE}\hat{i}_5^* \quad (5)$$

$$ACBD \rightarrow l_{AC}\hat{i}_1^* + l_{CB}\hat{i}_3^* = l_{AD}\hat{i}_2^* + l_{DB}\hat{i}_4^* \quad (6)$$

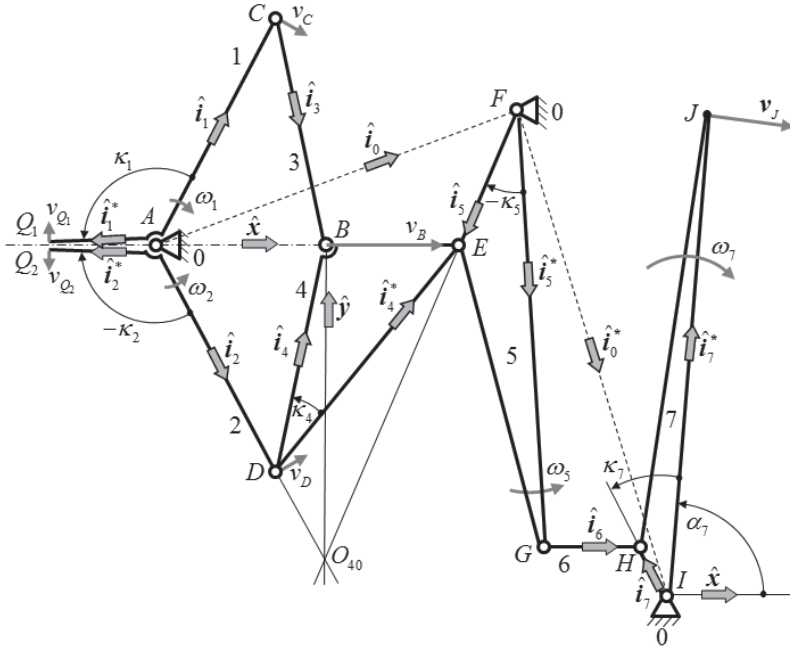


Fig. 4. Kinematic scheme, unit vector orientation and velocity vectors of the microgripper mechanism links

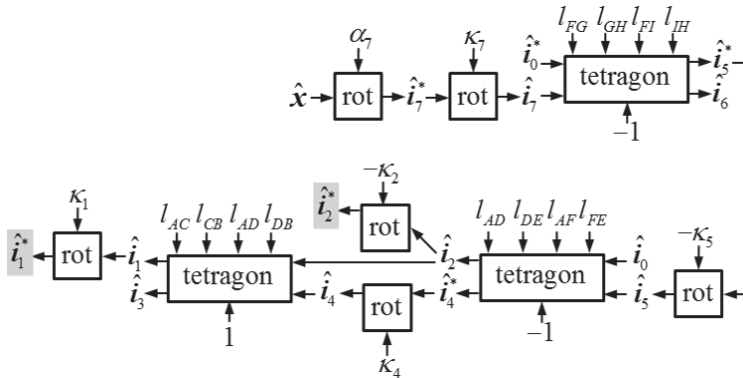


Fig. 5. An algorithm for determining the orientation of microgripper links

3.2. Gear ratio of the gripper mechanism

The angular movement ratios of the jaws k_{17} and k_{27} are the products of the gear ratio of the common part k_{s7} , which is the mechanism of reduction and gear ratio of the mechanism of the upper and lower jaw clamps k_{15} and k_{25} :

$$k_{17} = k_{15}k_{s7}, \quad k_{27} = k_{25}k_{s7}, \quad (7)$$

The ratio of k_{s7} is obtained from the differentials components of vector equation (4) projected onto the direction $\hat{\mathbf{i}}_6$:

$$k_{25} = \frac{d\alpha_2}{d\alpha_5} = \frac{l_{FE} [(\hat{\mathbf{i}}_4^* \times \hat{\mathbf{i}}_5) \cdot \hat{\mathbf{z}}]}{l_{AD} [(\hat{\mathbf{i}}_4^* \times \hat{\mathbf{i}}_2) \cdot \hat{\mathbf{z}}]} \quad (8)$$

The ratio of k_{15} and k_{25} is obtained analogously from equations (5) and (6):

$$k_{15} = \frac{d\alpha_1}{d\alpha_5} = \frac{l_{FE}}{l_{AC}} \frac{[(\hat{\mathbf{i}}_4^* \times \hat{\mathbf{i}}_5) \cdot \hat{\mathbf{z}}][(\hat{\mathbf{i}}_2 \times \hat{\mathbf{i}}_3) \cdot \hat{\mathbf{z}}]}{[(\hat{\mathbf{i}}_2 \times \hat{\mathbf{i}}_4^*) \cdot \hat{\mathbf{z}}][(\hat{\mathbf{i}}_3 \times \hat{\mathbf{i}}_1) \cdot \hat{\mathbf{z}}]} + \frac{l_{DB}l_{FE}}{l_{DE}l_{AC}} \frac{[(\hat{\mathbf{i}}_2 \times \hat{\mathbf{i}}_5) \cdot \hat{\mathbf{z}}][(\hat{\mathbf{i}}_3 \times \hat{\mathbf{i}}_4) \cdot \hat{\mathbf{z}}]}{[(\hat{\mathbf{i}}_2 \times \hat{\mathbf{i}}_4^*) \cdot \hat{\mathbf{z}}][(\hat{\mathbf{i}}_3 \times \hat{\mathbf{i}}_1) \cdot \hat{\mathbf{z}}]} \quad (9)$$

$$k_{25} = \frac{d\alpha_2}{d\alpha_5} = \frac{l_{FE} [(\hat{\mathbf{i}}_4^* \times \hat{\mathbf{i}}_5) \cdot \hat{\mathbf{z}}]}{l_{AD} [(\hat{\mathbf{i}}_4^* \times \hat{\mathbf{i}}_2) \cdot \hat{\mathbf{z}}]} \quad (10)$$

The gear ratio of the linear motion of jaws Q_1 and Q_2 with reference to the movement of point J of lever 7:

$$k_{Q_1J} = \frac{dy_{Q_1}}{dx_J} = -k_{17} \frac{l_{AQ_1} (\hat{\mathbf{x}} \cdot \hat{\mathbf{i}}_1^*)}{l_{IJ} (\hat{\mathbf{y}} \cdot \hat{\mathbf{i}}_7^*)} \quad (11)$$

$$k_{Q_2J} = \frac{dy_{Q_2}}{dx_J} = -k_{27} \frac{l_{AQ_2} (\hat{\mathbf{x}} \cdot \hat{\mathbf{i}}_2^*)}{l_{IJ} (\hat{\mathbf{y}} \cdot \hat{\mathbf{i}}_7^*)} \quad (12)$$

4. Results and conclusions

The theoretical values of the gear ratios presented in Table 1 were obtained on the basis of equations (11) and (12) taking into account the measured dimensions of the printed mechanism. Graphs of transversal points Q_1 and Q_2 were measured transverse to the axis of symmetry using a digital microscope with a magnification of 200 as a function of the displacement of point J , the motion of which was forced and simultaneously measured by

a micrometre screw. Measurements were made during closing and next during opening the jaws. The coefficients of inclination of the trends lines presented in Figs. 6 and 7 were adopted as the values of the measured ratios.

Table 1. Gear ratios

| | Upper jaw k_{Q_1J} [-] | Lower jaw k_{Q_2J} [-] |
|--------------|--------------------------|--------------------------|
| | Theoretical | |
| | $4.473 \cdot 10^{-3}$ | $-4.397 \cdot 10^{-3}$ |
| | Measured | |
| closing jaws | $3.026 \cdot 10^{-3}$ | $-2.990 \cdot 10^{-3}$ |
| opening jaws | $2.867 \cdot 10^{-3}$ | $-2.932 \cdot 10^{-3}$ |

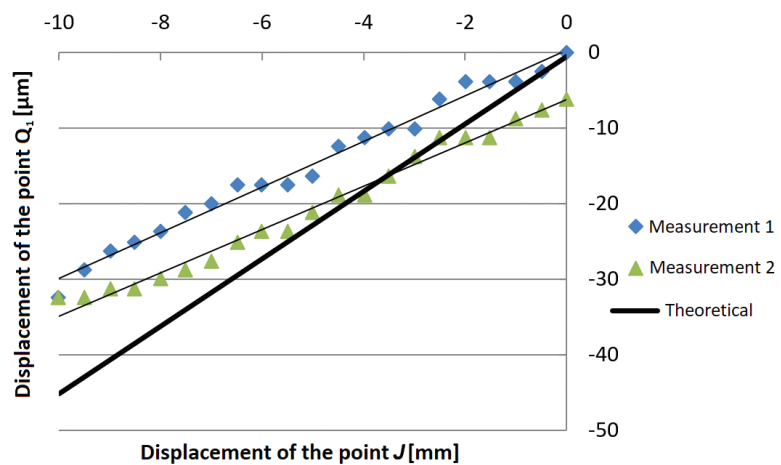


Fig. 6. Movement of the upper jaw point Q_1 as a function of point J of lever 7

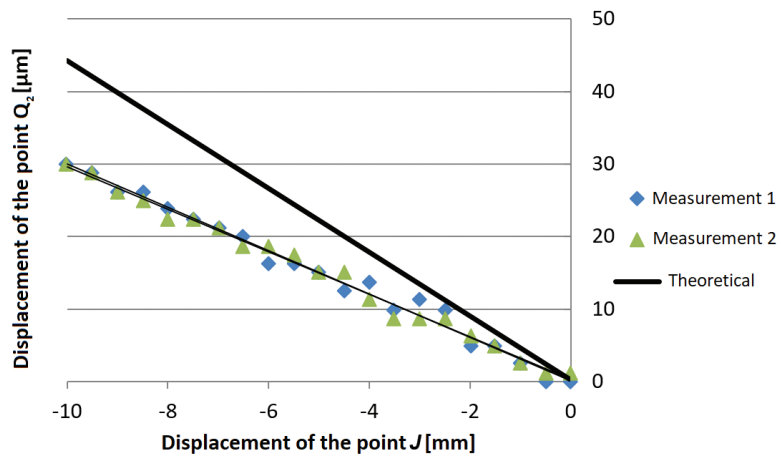


Fig. 7. Movement of the lower jaw point Q_2 as a function of junction point J of lever 7

Figure 8 presents a graph of the transverse differences between the coordinates of the pair of jaw points Q_1 and Q_2 . As a measure of the symmetry error of movement of the jaws, the largest distance of the measured difference from the trend line parallel to the axis of abscissae was assumed:

$$\delta = \max \left| Q_{1i}^y - Q_{2i}^y - \text{const} \right| \quad (13)$$

where:

$i = 1 \dots n$, n – number of measurements.

For distance change between the points of jaws Q_1 and Q_2 in the range of $90 \mu\text{m}$, the error of movement symmetry is $\delta = 1.6 \mu\text{m}$.

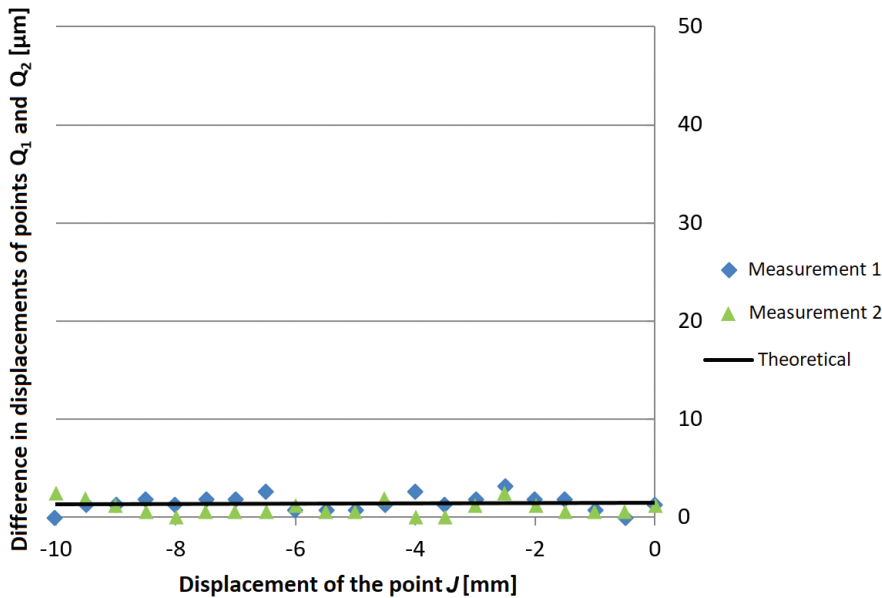


Fig. 8. Differences in the displacement of jaw points Q_1 and Q_2 as a function of point J displacement (lever 7)

The monolithic gripper mechanism is described as a lever mechanism with rotary joints in the constrictions. For the theoretical calculations, a constant distance between the centres of joints and negligibly small deformations of the lever were assumed. Theoretical gear ratios for the gripper jaws points depend on the variable products of the unit vectors. Mixed products thus formulated appear in the numerators and denominators of expressions into gears ratios, showing the influence of relative angular settings of the unit vectors on the gear ratios. Similarly, one can assess the influence of the dimensions of the levers forming the gripper mechanism.

The small range of movement of the mechanism causes the variable gear ratio functions to have a practically constant value. It has been found that changes in the measured displacements of the gripper jaw points are almost linear, but their values are clearly lower than the theoretical

values. Taking into account the material from which the mechanism was made, this is the expected effect, considering the relatively high susceptibility of the material. A short delay in the mechanism activation was found; this could not be measured by the available equipment.

The highest percentage deviation of the centre between the points of the gripper jaws from the trend line, related to the maximal opening of the jaws is equal 1.8%.

The use of PLA material is convenient as it is easy to manufacture and is suitable for prototype structures, the task of which is to qualitatively confirm the properties of the mechanism. The next stage of work will be the assessment of the performance of a monolith made of a material with greater homogeneity, e.g. steel. With more precise material parameters, it is possible to make precise quantitative calculations based on FEM analysis.

In the case of future constructions, it seems advisable to introduce the regulation of the permanent narrowing positions as this will enable the compensation of monolith errors.

References

- [1] Vijayasai A.P., Sivakumar G., Mulsow M., Lacouture S., Holness A., Dallas T.E., *Haptic controlled three degree-of-freedom microgripper system for assembly of detachable surface-micromachined MEMS*, Sensors and Actuators A: Physical 179/2012, 328–336.
- [2] Anis Y.H., Holl M.R., Meldrum D., *Automated vision-based selection and placement of single cells in microwell array formats*, 4th IEEE Conference on Automation Science and Engineering, 23–26 August 2008, 315–320.
- [3] Geng R.-R., Mills J.K., Yao Z.-Y., *Design and analysis of a novel 3-DOF spatial parallel microgripper driven by LUMs*, Robotics and Computer-Integrated Manufacturing 42/2016, 147–155.
- [4] Belfiore N.P., Simeone P., *Inverse kinetostatic analysis of compliant four-bar linkages*, Mechanism and Machine Theory 69/2013, 350–372.
- [5] Kim J.-J., Choi Y.-M., Ahn D., Hwang B., Gweon D.-G., Jeong J., *A millimeter-range flexure-based nano-positioning stage using a self-guided displacement amplification mechanism*, Mechanism and Machine Theory 50/2012, 109–120.
- [6] AbuZaiter A., Nafea M., Sultan Mohamed Ali M., *Development of a shape-memory-alloy micromanipulator based on integrated bimorph microactuators*, Mechatronics 38/2016, 16–28.
- [7] Kim K., Liu X., Zhang Y., Sun Y., *Nanonewton force-controlled manipulation of biological cells using a monolithic MEMS microgripper with two-axis force feedback*, Journal of Micromechanics and Microengineering 18/2008, 1–8.
- [8] Cecchi R., Verotti M., Capata R., Dochsharov A., Broggiato G.B., Crescenzi R., Balucani M., Natali S., Razzano G., Lucchese F., Bagolini A., Bellutti P., Sciubba E., Belfiore N.P., *Development of Micro-Grippers for Tissue and Cell Manipulation with Direct Morphological Comparison*, Micromachines 6/2015, 1710–1728.
- [9] Chace M.A., *Development and application of vector mathematics for kinematic analysis of three-dimensional mechanisms*, Doctoral dissertation, University of Michigan, 1964.



